Published OnlineFirst June 28, 2016; DOI: 10.1158/2159-8290.CD-15-0675

RESEARCH ARTICLE

Triggering the TCR Developmental Checkpoint Activates a Therapeutically Targetable Tumor Suppressive Pathway in T-cell Leukemia

Amélie Trinquand[1], Nuno R. dos Santos[2,3], Christine Tran Quang[3,4], Francesca Rocchetti[3,4], Benedetta Zaniboni[3,4], Mohamed Belhocine[1,5], Cindy Da Costa de Jesus[3,4], Ludovic Lhermitte[1], Melania Tesio[1], Michael Dussiot[6], François-Loïc Cosset[7], Els Verhoeyen[7,8], Françoise Pflumio[9], Norbert Ifrah[10], Hervé Dombret[11], Salvatore Spicuglia[5], Lucienne Chatenoud[12], David-Alexandre Gross[12], Olivier Hermine[6,13], Elizabeth Macintyre[1], Jacques Ghysdael[3,4], and Vahid Asnafi[1]

Published OnlineFirst June 28, 2016; DOI: 10.1158/2159-8290.CD-15-0675

ABSTRACT Cancer onset and progression involves the accumulation of multiple oncogenic hits, which are thought to dominate or bypass the physiologic regulatory mechanisms in tissue development and homeostasis. We demonstrate in T-cell acute lymphoblastic leukemia (T-ALL) that, irrespective of the complex oncogenic abnormalities underlying tumor progression, experimentally induced, persistent T-cell receptor (TCR) signaling has antileukemic properties and enforces a molecular program resembling thymic negative selection, a major developmental event in normal T-cell development. Using mouse models of T-ALL, we show that induction of TCR signaling by high-affinity self-peptide/MHC or treatment with monoclonal antibodies to the CD3ε chain (anti-CD3) causes massive leukemic cell death. Importantly, anti-CD3 treatment hampered leukemogenesis in mice transplanted with either mouse- or patient-derived T-ALLs. These data provide a strong rationale for targeted therapy based on anti-CD3 treatment of patients with TCR-expressing T-ALL and demonstrate that endogenous developmental checkpoint pathways are amenable to therapeutic intervention in cancer cells.

SIGNIFICANCE: T-ALLs are aggressive malignant lymphoid proliferations of T-cell precursors characterized by high relapse rates and poor prognosis, calling for the search for novel therapeutic options. Here, we report that the lineage-specific TCR/CD3 developmental checkpoint controlling cell death in normal T-cell progenitors remains switchable to induce massive tumor cell apoptosis in T-ALL and is amenable to preclinical therapeutic intervention. *Cancer Discov; 6(9); 972–85. ©2016 AACR.*

See related commentary by Lemonnier and Mak, p. 946.

INTRODUCTION

Developmental checkpoints in stem/progenitor cells are critical to their determination, commitment, and differentiation into distinct lineages. Cancer cells often retain expression of lineage-specific checkpoint proteins, but their potential impact in cancer remains elusive (1). T lymphocytes mature in the thymus following a highly orchestrated developmental process that entails the successive rearrangements and expression of T-cell receptor (TCR) genes. TCRδ rearrangements first occur at the $CD5^+$, $CD1a^-$, CD4/8 double-negative (DN) stage, followed by concurrent TCRγ and TCRβ rearrangements coinciding with CD1a expression. Although productive TCRγ and TCRδ rearrangements will determine the assembly of a TCRγδ, a complete productive TCRβ gene rearrangement will first allow surface expression of a pre-TCR complex formed by the assembly of the TCRβ chain with a pre-Tα (pTα) invariant chain. Pre-TCR surface expression is a critical checkpoint for developing αβ T-cell precursors to expand and mature into CD4/CD8 double-positive (DP) cortical thymocytes and for the initiation of Vα–Jα rearrangements. These rearrangements continue until a TCRα chain is formed that can associate with the already formed TCRβ chain to assemble a complete mature TCRαβ at the cell surface (2, 3). Cell surface expression of the TCR is a critical developmental checkpoint in establishing MHC restriction and in shaping the immunologic repertoire. Low-affinity recognition of self-peptide/major histocompatibility complexes (self-pMHC) presented by thymic epithelial cells to the TCR of $CD4^+CD8^+$ DP cortical thymocytes transduces positive selection signals and commitment to

[1]Université Paris Descartes Sorbonne Cité, Institut Necker-Enfants Malades (INEM), Institut national de recherche médicale (INSERM) U1151, and Laboratory of Onco-Hematology, Assistance Publique-Hôpitaux de Paris (AP-HP), Hôpital Necker Enfants-Malades, Paris, France. [2]Centre for Biomedical Research (CBMR), University of Algarve, Faro, Portugal. [3]Institut Curie, PSL Research University, CNRS UMR 3348, Orsay, France. [4]Université Paris Sud, Université Paris-Saclay, CNRS UMR 3348, Orsay, France. [5]Technological Advances for Genomics and Clinics (TAGC), INSERM U1090, Université de la Méditerranée, Marseille, France. [6]INSERM UMR 1163 and CNRS ERL 8654, Laboratory of Cellular and Molecular Mechanisms of Hematological Disorders and Therapeutic Implications, Laboratory of Excellence GR-Ex, Imagine Institute and Paris Descartes University, Sorbonne Paris Cité, Paris, France. [7]CIRI, EVIR Team, INSERM U1111, CNRS UMR 5308, Université de Lyon-1, ENS de Lyon, Lyon, France. [8]INSERM U1065, C3M, Equipe "Contrôle Métabolique des Morts Cellulaires," Nice, France. [9]Laboratoire des Cellules Souches Hématopoïétiques et Leucémiques, UMR 967, INSERM, Commissariat à l'Energie Atomique, Université Paris Diderot, Université Paris 11, Institut de Radiobiologie Cellulaire et Moléculaire, équipe labellisée Ligue Nationale contre le Cancer, Fontenay-aux-Roses, France. [10]PRES LUNAM, CHU Angers service des Maladies du Sang et INSERM U892, Angers, France. [11]Université Paris 7, Hôpital Saint-Louis, AP-HP, Department of Hematology and Institut Universitaire d'Hématologie, Paris, France. [12]Institut Necker Enfants Malades, INSERM U1151, CNRS UMR 8253, Hôpital Necker-Enfants Malades, Paris, France, and Université Paris Descartes Sorbonne Paris Cité, Paris, France. [13]Department of Clinical Hematology, Hôpital Necker, Assistance publique hôpitaux de Paris, Paris, France.

Note: Supplementary data for this article are available at Cancer Discovery Online (http://cancerdiscovery.aacrjournals.org/).

A. Trinquand, N.R. dos Santos, and C. Tran Quang contributed equally to this article.

Current address for Nuno R. dos Santos: i3S-Instituto de Investigaçao e Inovaçao em Saude, IPATIMUP, Universidade do Porto, Porto, Portugal.

Corresponding Authors: Vahid Asnafi, Hôpital Necker Enfants-Malades, Laboratoire d'onco-hématologie, 149 rue de Sèvres, 75015 Paris, France. Phone: 144-49-49-14; Fax: 144-38-17-45; E-mail: vahid.asnafi@aphp.fr; and Jacques Ghysdael, Signalisation Cellulaire et Oncogenèse, UMR3348 CNRS-Institut Curie, Centre Universitaire, Bat 110, 91405 Orsay, France. Phone: 169-86-31-52; 169-86-94-29; E-mail: jacques.ghysdael@curie.fr

doi: 10.1158/2159-8290.CD-15-0675

Published OnlineFirst June 28, 2016; DOI: 10.1158/2159-8290.CD-15-0675

either the CD4 or CD8 lineages. DP thymocytes not receiving these signals die by lack of stimulation, whereas those that recognize self-pMHC with high affinity undergo TCR-mediated apoptosis and negative selection (4, 5).

T-cell acute lymphoblastic leukemia (T-ALL) results from the leukemic transformation of thymic cell precursors and their arrest at specific stages of differentiation (6–8). Despite recent and extensive insights into the molecular and cellular mechanisms responsible for T-ALL onset and progression, survival rates remain around 50% and 70% in adult and pediatric cases, respectively, calling for the search for novel therapeutic options. In T-ALL, leukemic transformation of maturing thymocytes is caused by a multistep pathogenesis involving numerous genetic abnormalities that drive normal T cells into uncontrolled cell growth and clonal expansion. T-ALL is classified into subgroups based upon exclusive gene rearrangement and/or expression of a limited set of transcription factors including TAL1, LMO1/2, TLX1/3, associated with the specific arrest at distinct stages of T-cell differentiation (8–10). Across these molecular subclasses, a number of other recurrent genetic alterations are found, including inactivation of the *CDKN2A* tumor suppressor locus, NOTCH1 pathway activating mutations, and many others (reviewed in ref. 11).

In this study, we hypothesized that tissue homeostatic regulators may be amenable to reactivation in tumor cells and demonstrate that experimentally induced TCR signaling in T-ALL induces cell death and a molecular program similar to negative selection of thymic T-cell progenitors. Importantly, switching on this TCR-induced cell death program dominates the multiple antiapoptotic and proproliferative mechanisms controlled by the oncogenes and altered tumor suppressors of T-ALL. These data provide a strong rationale for targeted therapy based upon anti-CD3 treatment in TCR-expressing T-ALL.

RESULTS

T-ALL Development Is Hampered by Antigen-Presenting Cell-Mediated TCR Stimulation

To investigate the role of TCRαβ activation by a defined antigen in T-ALL, we stably expressed the negatively selecting Marilyn TCR-HY (Vα1.1Vβ6) specific for the HY male antigen (DBY) in the TCR-negative ALL-SIL T-ALL cell line. *In vitro* coculture of ALL-SIL/TCR-HY cells with splenocytes pulsed with increasing doses of DBY peptide, but not the unrelated OVA peptide, induced leukemic cell death (Fig. 1A and quantified in Fig. 1B). DBY peptide did not induce apoptosis of parental TCR-negative ALL-SIL cells nor of ALL-SIL/TCR-HY cells cultured in the absence of MHC-restricted antigen-presenting syngeneic splenocytes (Fig. 1A). These data demonstrate that TCR activation by the cognate peptide–MHC complex results in T-ALL cell death. To determine the effect of persistent TCR stimulation on T-cell leukemogenesis, we generated double transgenic mice (hereafter referred to as TEL-JAK2/TCR-HY mice) expressing the TEL–JAK2 fusion oncogene (12) and the Marilyn TCR-HY (13) in lymphoid progenitors. As compared with TEL-JAK2/TCR-HY double transgenic females, which developed rapid and fully penetrant T-ALL, the majority of TEL-JAK2/TCR-HY males either failed to become leukemic or developed leukemia with markedly delayed latency (Fig. 2A). Flow cytometry analysis showed that of seven diseased male mice analyzed, two developed B-cell lymphoma/leukemia whereas five developed T-cell leukemia (Fig. 2B). Strikingly, in the five T-ALL cases, transgenic

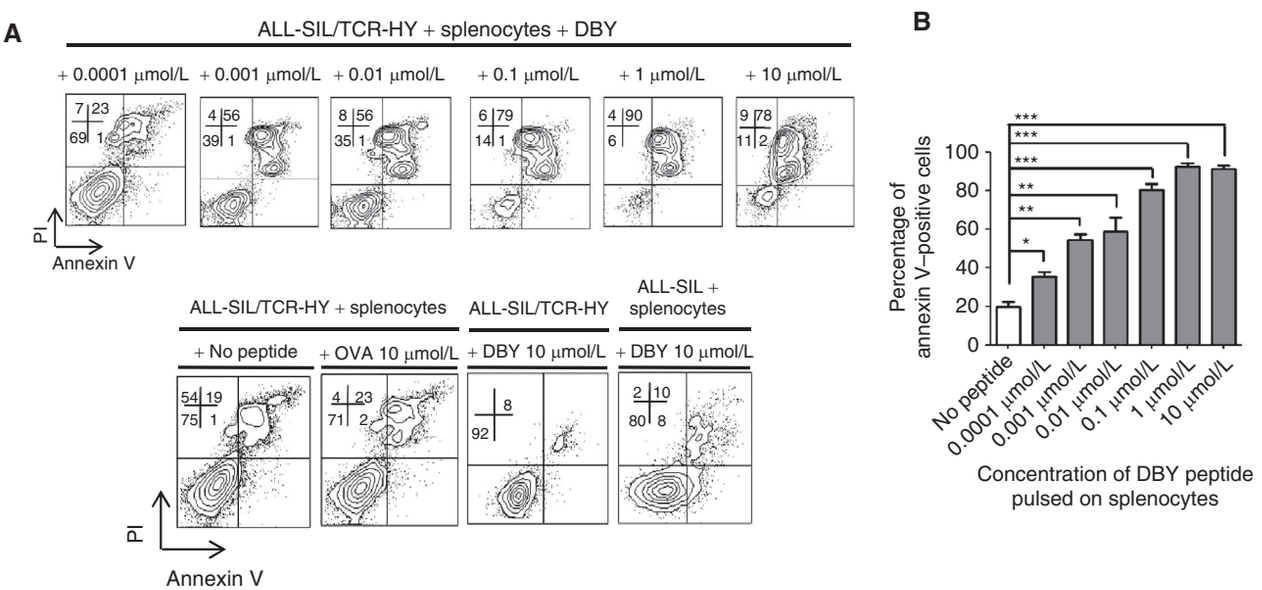

Figure 1. TCR stimulation by antigen-presenting cells induces ALL-SIL/TCR-HY cell death. **A,** ALL-SIL/TCR-HY cells were cocultured for 3 days with irradiated female splenocytes pulsed with the indicated doses of cognate DBY peptide (top), as compared with control conditions (bottom): absence of DBY (no peptide), presence of a noncognate peptide (+ OVA 10 μmol/L), presence of DBY without splenocytes (+ DBY 10 μmol/L), or ALL-SIL parental cells stimulated with splenocytes and DBY. Apoptosis was analyzed by annexin V and propidium iodide (PI) staining. Dot plots were gated on ALL-SIL cells. **B,** graphical representation of apoptosis level in 3 independent experiments as described in **A** (***$P \leq 0.0001$, $0.001 \leq$ **$P < 0.0001$, $0.05 <$ *$P < 0.001$).

Published OnlineFirst June 28, 2016; DOI: 10.1158/2159-8290.CD-15-0675

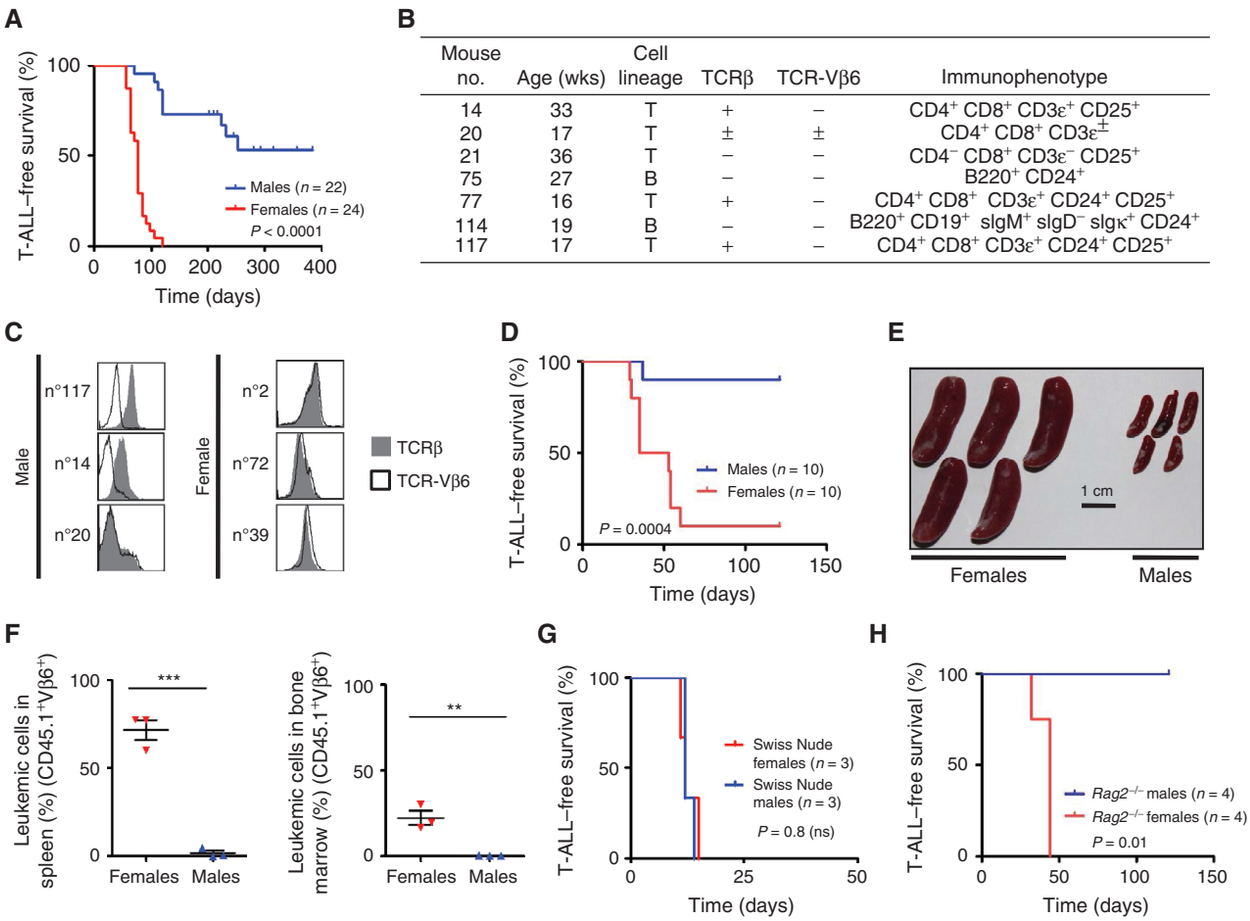

Figure 2. TCR-HY stimulation prevents T-ALL development. **A,** Kaplan–Meier survival curves for male and female TEL-JAK2/TCR-HY mice. **B,** leukemic cell-surface immunophenotype of male TEL-JAK2/TCR-HY mice. **C,** flow cytometry analysis of TCRβ and TCR-Vβ6 surface expression on leukemic cells from three male and three female TEL-JAK2/TCR-HY mice that developed T-ALL. **D,** Kaplan–Meier survival curves for secondary female and male recipient syngeneic mice transplanted with female TEL-JAK2/TCR-HY leukemic cells. **E,** spleens from recipient female and male mice transplanted as described in **D** but sacrificed 17 days later. **F,** leukemic burden analysis of spleen (left) and bone marrow (right) of mice transplanted as in **D** but sacrificed at the time females became terminally ill. **, $P < 0.01$; ***, $P < 0.001$. **G,** Kaplan–Meier survival curves of Swiss Nude allogeneic mice transplanted with female TEL-JAK2/TCR-HY leukemic cells (ns, nonsignificant). **H,** Kaplan–Meier T-ALL–free survival curves of *Rag2*$^{-/-}$ syngeneic mice transplanted with female TEL-JAK2/TCR-HY leukemic cells.

TCR-Vβ6 cell surface expression was low or absent, and leukemic cells often expressed either no TCR or an endogenous TCR (Fig. 2C), suggesting that in these mice, expression of TCR-HY, but not of non–HY-specific TCR complexes, was counterselected during leukemogenesis. We conclude that self-antigen TCR stimulation suppresses thymocyte malignant transformation, thus delaying leukemogenesis in male mice.

To investigate whether delayed leukemogenesis in TEL-JAK2/TCR-HY male mice could be attributed to direct antigenic stimulation of TCR-expressing leukemic cells, female TEL-JAK2/TCR-HY CD45.1$^+$ T-ALL cells were transplanted to either female (HY-negative) or male (HY-positive) syngeneic CD45.2$^+$ recipient mice. As compared with female recipients, which rapidly developed fatal T-ALL, most recipient males failed to develop leukemia and survived longer (Fig. 2D). In contrast to male mice sacrificed simultaneously, female recipients presented high infiltration of CD45.1$^+$ leukemic cells in spleen, lymph nodes, and bone marrow (Fig. 2E and F, and data not shown). The resistance of male mice to TEL-JAK2/TCR-HY–induced leukemogenesis depended on HY antigen MHC presentation but not upon an adaptive immune response, because T-ALL developed efficiently following transplantation of TEL-JAK2/TCR-HY leukemic cells in male allogeneic immunodeficient recipient mice (Fig. 2G), but not in male syngeneic immunodeficient recipients (Fig. 2H). These results show that the TCR anti-leukemic effect depends upon its stimulation by the cognate peptide–MHC complex.

Anti-CD3 Stimulation of ALL-SIL/TCR-HY Cells Induces TCR Signaling and Apoptosis

We next investigated whether anti-CD3 treatment could mimic TCR signaling to induce leukemic cell apoptosis. Unlike control ALL-SIL cells, TCR-HY–expressing cells underwent massive apoptosis when treated with anti-CD3/

Published OnlineFirst June 28, 2016; DOI: 10.1158/2159-8290.CD-15-0675

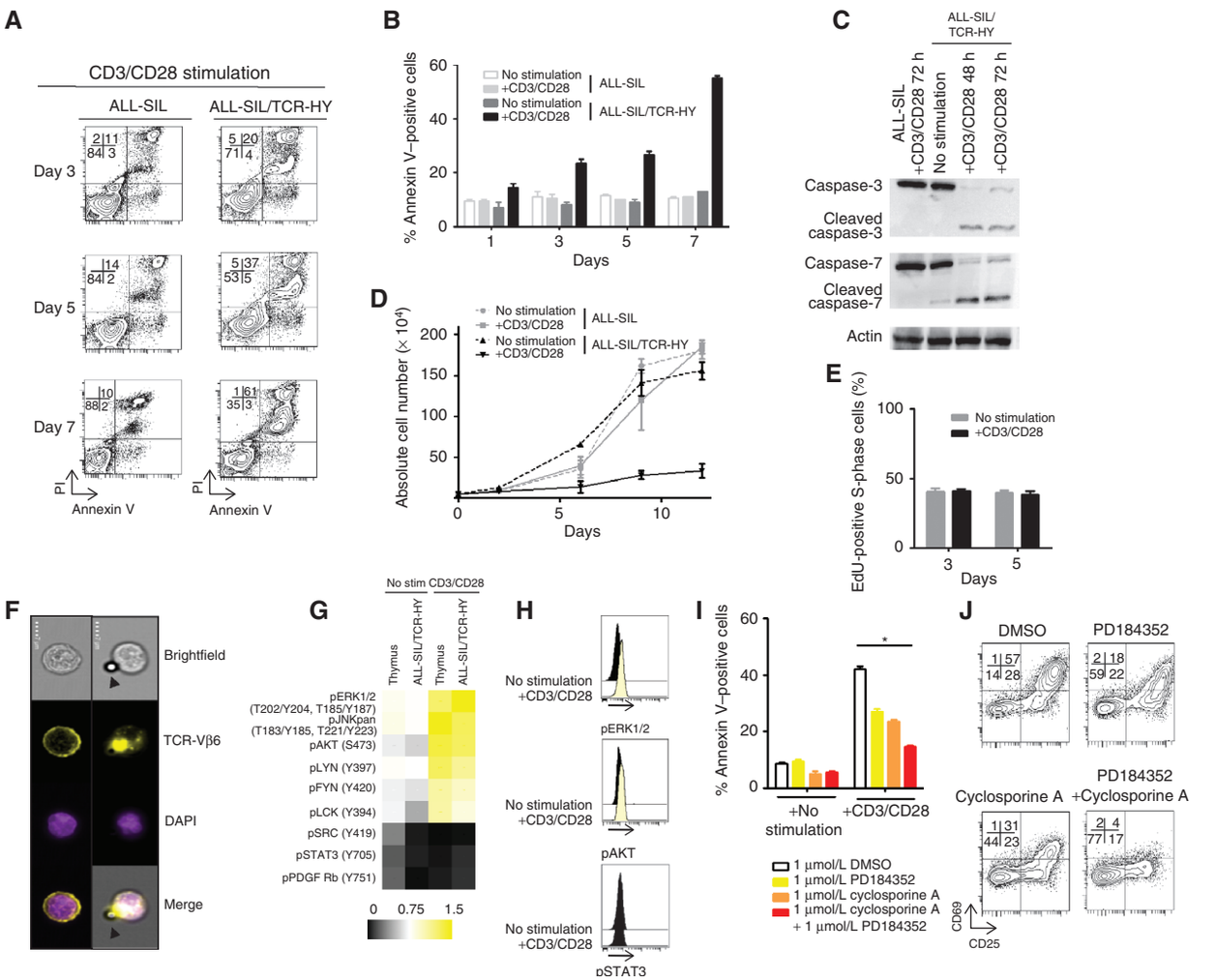

Figure 3. Anti-CD3 stimulation of ALL-SIL/TCR-HY cells induces TCR signaling and apoptosis. **A,** apoptosis detection by annexin V and PI staining of ALL-SIL and ALL-SIL/TCR-HY cells stimulated by anti-CD3/CD28–coated beads at the indicated time points. **B,** percentage of annexin V–positive ALL-SIL or ALL-SIL/TCR-HY cells either left unstimulated or stimulated by anti-CD3/CD28–coated beads for the indicated time. **C,** Western blot analysis of caspase-3 and caspase-7 cleavage in ALL-SIL and ALL-SIL/TCR-HY cells either left unstimulated or stimulated by anti-CD3/CD28–coated beads for 48 and 72 hours. Actin was used as a loading control. **D,** growth curve of unstimulated and anti-CD3/CD28–stimulated ALL-SIL and ALL-SIL/TCR-HY cells. **E,** percentage of unstimulated or anti-CD3/CD28–stimulated ALL-SIL/TCR-HY cells in the S-phase of the cell cycle as measured by EdU incorporation and 7-AAD staining of DNA. **F,** ImageStream flow cytometry imaging of ALL-SIL/TCR-HY single cells showing the recruitment of TCR-Vβ6 to a contacting anti-CD3–coated bead (arrowhead; each row shows one cell in bright field, phycoerytrin, and DAPI fluorescence and merge of three channels, ×40). **G,** heat map representation of the normalized ratio of intensity of indicated phosphorylated (p) proteins in Proteome Profiler Human phosphokinase array, representative of two experiments. **H,** pERK, pAKT, and pSTAT3 expression detected by flow cytometry in nonstimulated (top line in each panel) or 30-minute anti-CD3/CD28–stimulated (bottom line) ALL-SIL/TCR-HY cells. **I,** percentage of annexin V–positive unstimulated (left) or anti-CD3/CD28–stimulated (right) ALL-SIL/TCR-HY cells at day 5, in the presence of indicated signaling pathway inhibitors. *, $P < 0.05$. **J,** inhibitory effects of indicated drugs on expression of T-cell activation markers (CD25 and CD69) in anti-CD3/CD28–stimulated ALL-SIL/TCR-HY for 2 days.

anti-CD28 or anti-CD3 alone (data not shown), as revealed by increased levels of cell-surface Annexin V, increased cleavage of caspase-3 and -7, and reduced cell expansion (Fig. 3A–D). Importantly, anti-CD3/anti-CD28 treatment did not affect cell-cycle progression *per se* (Fig. 3E and data not shown). To investigate the signaling properties of the mouse TCR-HY complex in human leukemic ALL-SIL cells, we first demonstrated that CD3 cross-linking induced TCR clustering at the ALL-SIL cell surface (Fig. 3F). Next, phosphokinase-array analysis of anti-CD3/anti-CD28–stimulated ALL-SIL/TCR-HY and normal human DP thymocytes showed increased phosphorylation of overlapping TCR signaling components, including the key downstream second messengers ERK, JNK, and AKT (Fig. 3G). Anti-CD3–induced phosphorylation of these proteins, and not of the cytokine signaling STAT3 protein, was confirmed by flow cytometry (Fig. 3H and data not shown). Of note, inhibition of TCR signaling by cyclosporine or the MEK kinase inhibitor PD184352 impaired anti-CD3–induced apoptosis and expression of the CD69 and CD25 T-cell activation markers (Fig. 3I and J). Together, these results indicate that the TCR/CD3 signaling module is functional in T-ALL cells, and that its activation leads to

Published OnlineFirst June 28, 2016; DOI: 10.1158/2159-8290.CD-15-0675

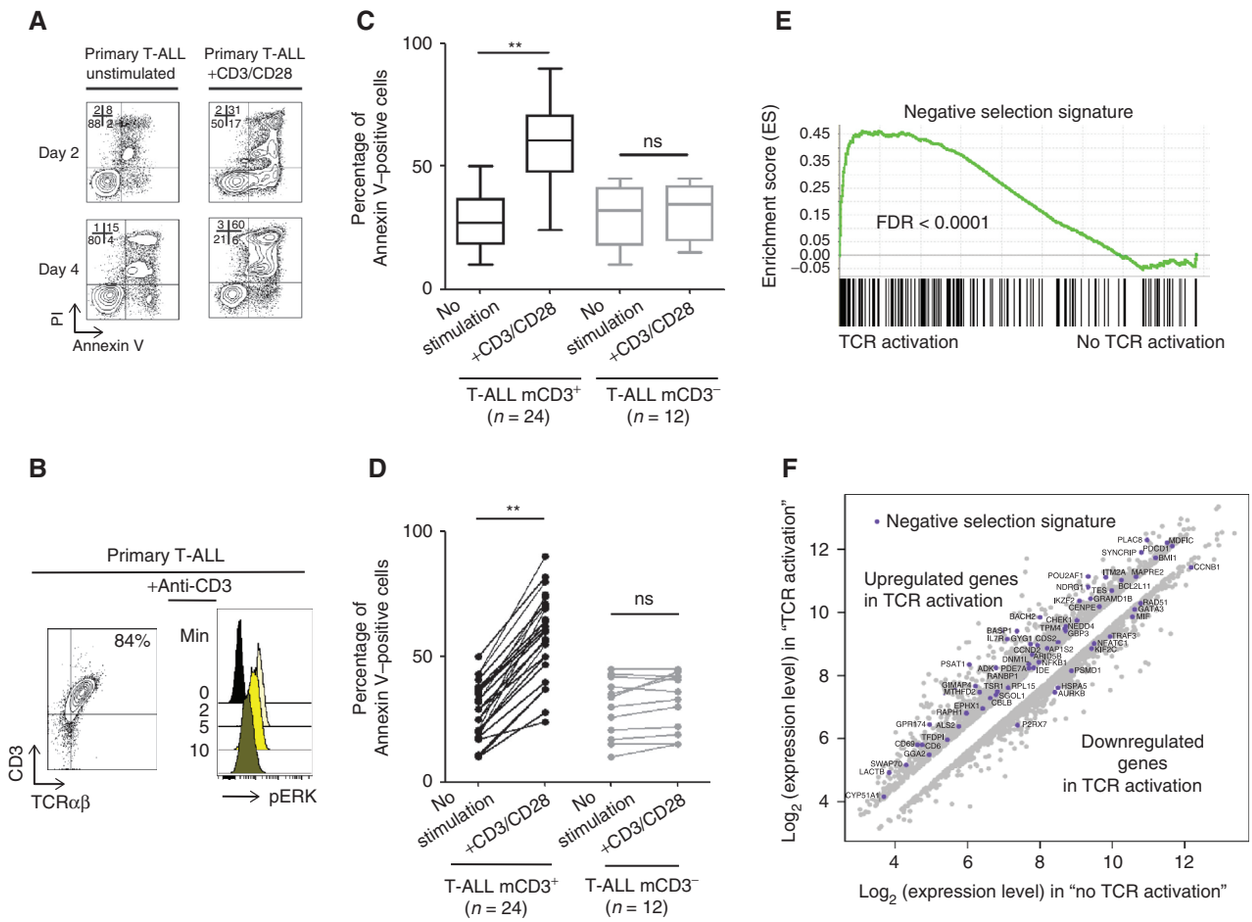

Figure 4. Anti-CD3 induces human primary T-ALL apoptosis *in vitro* and mimics thymic negative selection. **A,** apoptosis analysis of primary T-ALL cells (UPNT419) cocultured on OP9-DL1 cells with or without anti-CD3/CD28 stimulation for 2 or 4 days. **B,** flow cytometry analysis of the induction kinetics of ERK1/2 phosphorylation (right) upon anti-CD3 (OKT3) stimulation of surface TCR/CD3-positive primary T-ALL (UPNT419; left). **C,** box and whisker plot presentation of apoptosis induction for each individual TCR/CD3-positive primary, diagnostic T-ALL cells (24 cases) as compared with apoptosis induction for each individual TCR/CD3-negative primary T-ALL cells (12 cases) after 3 days of coculture on OP9-DL1 in the presence or absence of CD3/CD28 stimulation (**, $P < 0.0001$; ns, nonsignificant). **D,** before and after plot representation of the comparison of apoptosis induction in TCR/CD3-positive primary, diagnostic T-ALL cells (24 cases) versus TCR/CD3-negative primary T-ALL cells (12 cases) as described in **C** (**, $P < 0.0001$; ns, nonsignificant). **E,** GSEA of the negative selection gene signature (14) comparing the ALL-SIL transcriptome with or without TCR activation, showing an enrichment in the TCR activation transcriptome. **F,** scatter plot showing upregulated and downregulated genes in response to TCR activation in ALL-SIL cells. The negative clonal deletion gene expression signature is detailed.

apoptosis. Importantly, similar results were observed in primary T-ALL (Supplementary Fig. S1A–S1C).

Targeting CD3 *In Vitro* Induces Human Primary T-ALL Apoptosis and Mimics Thymic Negative Selection

To test whether anti-CD3 stimulation of TCR-expressing T-ALL diagnostic samples also induced apoptosis, primary human T-ALL cells (see Supplementary Table S1 for the immunophenotypic and genetic features of the diagnostic samples used) belonging to the major molecular oncogenic T-ALL subclasses were treated with anti-CD3/anti-CD28. Massive T-ALL apoptosis and TCR signaling activation were observed in TCR-expressing T-ALL but not in TCR-negative cases, regardless of their molecular oncogenic subtype (Fig. 4A–D). We next analyzed the transcriptional profiles of TCR-expressing ALL-SIL cells either unstimulated or after TCR stimulation and found in the ALL-SIL TCR-induced transcriptional profile a significant enrichment for the TCR-induced negative selection signature of normal thymic progenitors (ref. 14; Fig. 4E and F). This shows that T-ALL apoptosis induced by TCR stimulation is associated with signaling cues resembling those of TCR-induced negative selection in normal T-cell progenitors.

Mouse and Human T-ALL Development Is Hampered by TCR Stimulation with Agonistic Monoclonal Antibodies

To assess the therapeutic potential of TCR stimulation by anti-CD3 treatment *in vivo*, we first inoculated female syngeneic mice with transgenic TEL-JAK2/TCR-HY leukemic cells and the following day initiated treatment with either an

Published OnlineFirst June 28, 2016; DOI: 10.1158/2159-8290.CD-15-0675

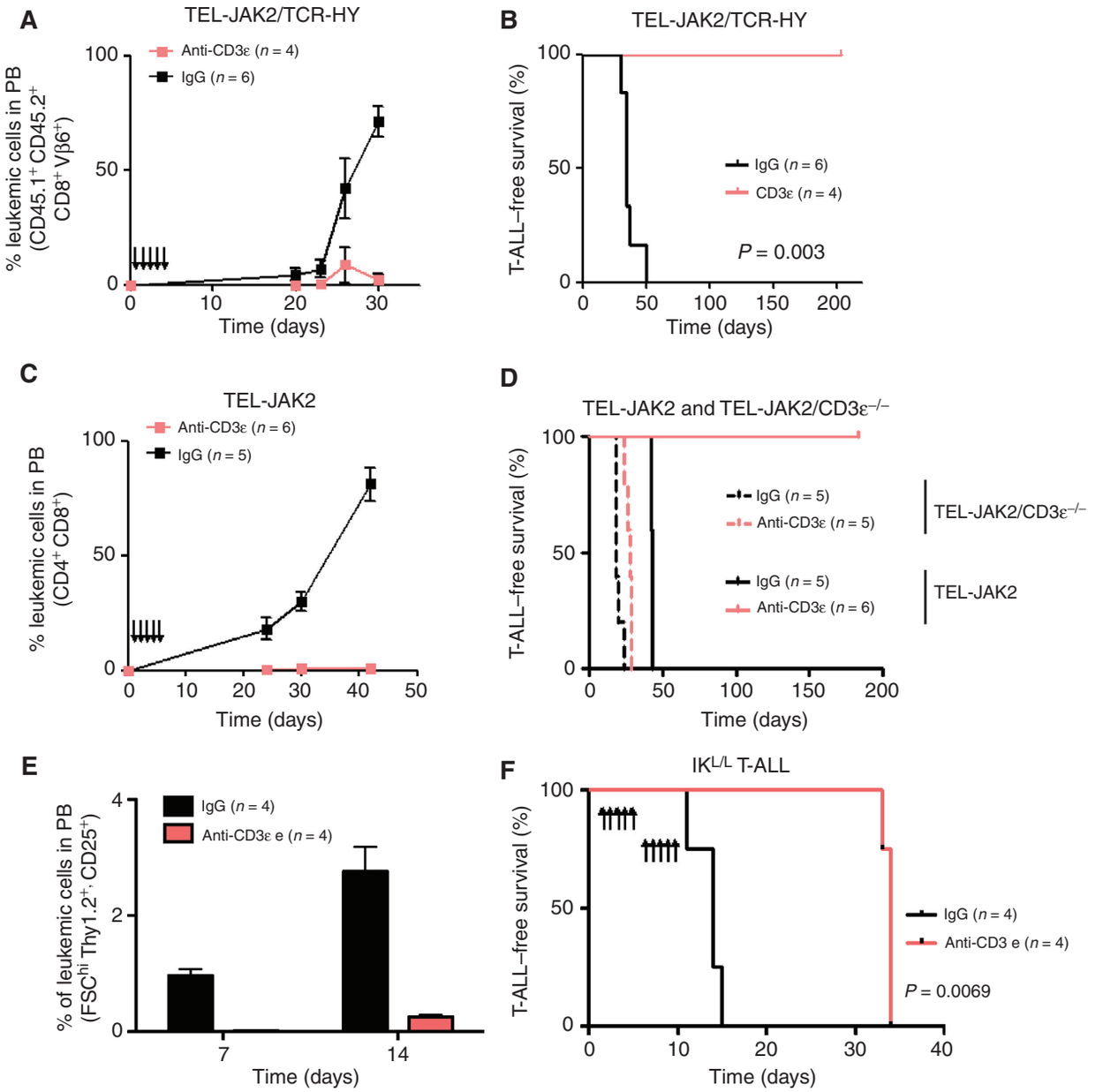

Figure 5. TCR stimulation by agonistic mAb *in vivo* administration inhibits mouse T-ALL development. **A** and **B,** percentage of TEL-JAK2/TCR-HY leukemic cells in peripheral blood (PB; **A**) and Kaplan–Meier survival curves (**B**) of female mice treated daily as indicated (arrows) with hamster anti-CD3 mAb or control IgG. **C,** percentage of TEL-JAK2 leukemic cells (expressing endogenous TCR) in peripheral blood leukocytes of mice that were treated daily with anti-CD3 or control hamster IgG. **D,** Kaplan–Meier survival curves of mice injected with either TEL-JAK2 leukemic cells (expressing endogenous TCR), or TEL-JAK2/CD3ε$^{-/-}$ leukemic cells and treated daily with anti-CD3 or control hamster IgG. **E,** percentage of IK$^{L/L}$ leukemic cells in peripheral blood leukocytes defined as FSC^{hi}, Thy1.2^{+} CD25^{+} in control IgG or anti-CD3–treated NOD/SCID/$\gamma^{c-/-}$ (NSG) mice at the indicated time point. **F,** Kaplan–Meier survival curves of NSG mice injected with IK$^{L/L}$ leukemic cells treated with hamster anti-CD3 mAb or control IgG as indicated.

anti-CD3ε monoclonal antibody (mAb) known to induce negative selection in normal thymic progenitors (15) or an isotypic control antibody for 5 consecutive days. Strikingly, both peripheral blood leukemia and fatal disease were impaired in anti-CD3–treated mice, whereas all mice treated with control antibody rapidly succumbed to leukemia (Fig. 5A and B). Importantly, treatment with anti-CD3 mAb was also effective against TEL-JAK2 T-ALL cells expressing endogenous surface TCRαβ (Fig. 5C and D). Of note, anti-CD3 treatment only marginally prolonged the leukemia-free survival of mice infused with CD3ε$^{-/-}$ TEL-JAK2 T-ALL cells (Fig. 5D). This shows that the extended survival seen in anti-CD3–treated mice inoculated with CD3ε$^{+/+}$ TEL-JAK2 T-ALL (Fig. 5D) critically depends upon engagement of the TCR/CD3 complex

Published OnlineFirst June 28, 2016; DOI: 10.1158/2159-8290.CD-15-0675

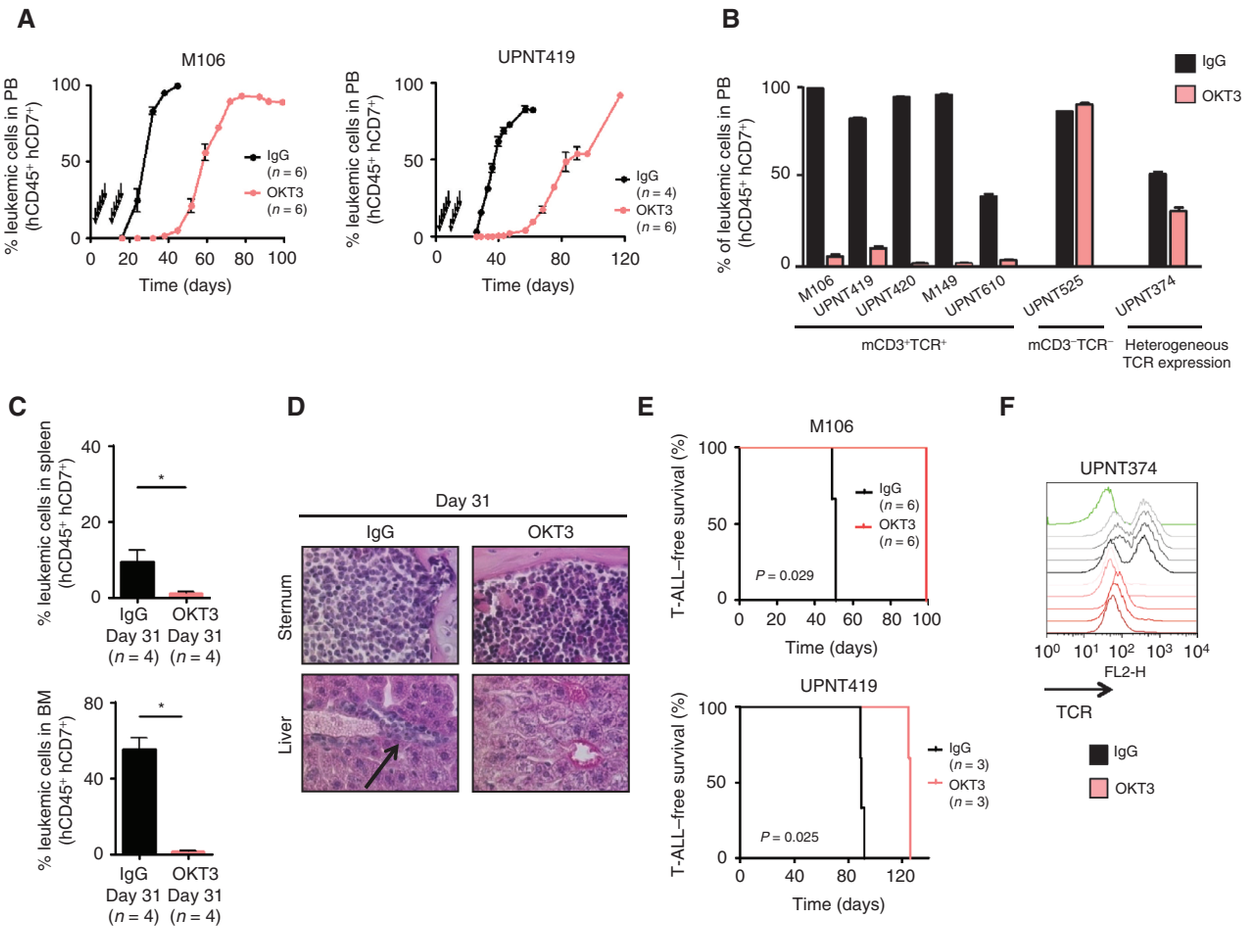

Figure 6. TCR stimulation by *in vivo* administration of agonistic mAb in a preventive setting inhibits human T-ALL development. **A,** flow cytometry monitoring of leukemia burden in peripheral blood (PB) from NSG mice injected with human T-ALL M106 and UPNT419 and treated daily with either OKT3 or an isotype control IgG (arrows). **B,** tumor burden in peripheral blood of NSG mice injected with human primary T-ALL cells either mCD3/TCR positive: M106 ($n = 6$ in each group), UPNT419 ($n = 5$ in each group), UPNT420 ($n = 5$ in each group), M149 ($n = 6$ in each group) UPNT610 ($n = 5$ in each group), or mCD3/TCR negative: UPNT525 ($n = 5$ in each group), or heterogeneous for CD3/TCR expression: UPNT374 ($n = 5$ in each group). Mice were treated with either control IgG or OKT3 in a preventive setting. Data show tumor burden in peripheral blood analyzed at the time when IgG-treated mice were moribund and sacrificed, except for UPTN610. For all TCR$^+$ leukemias, the P value was <0.0001. **C,** leukemia burden in spleen (top) and bone marrow (BM; bottom) of control and OKT3-treated mice that were sacrificed when IgG-treated control mice were leukemic (day 31 of **A**). *, $P = 0.0409$ (spleen); *, $P = 0.011$ (BM). **D,** H&E-stained bone marrow and liver sections of mice analyzed in **B**. The arrow indicates infiltrating cells in liver perivascular spaces and sinusoids. **E,** Kaplan–Meier survival curves of NSG mice transplanted with M106 and UPNT419 human T-ALL cells analyzed as in **A**. **F,** flow cytometry analysis of cell surface TCR in leukemic BM cells of NSG mice xenografted with T-ALL UPNT374 treated with either control IgG (black/gray tracings) or OKT3 (red to pink tracings) at the time of sacrifice. Green tracing shows staining with the control isotypic antibody.

expressed by leukemic cells. To ensure that the results were not restricted to this particular model of activated tyrosine kinase–induced T-ALL, we extended these analyses to *Ikzf1/Ikaros*-mutant–induced T-ALL. Although *Ikaros* is rarely found mutated in T-ALL, recent evidence points to a suppressive function of *Ikaros* in NOTCH-mutated T-ALL cells (16). Treatment with anti-CD3 mAb inhibited leukemia expansion in this model (Fig. 5E), which translated into increased survival of anti-CD3–treated mice (Fig. 5F).

Finally and most importantly, we investigated whether anti-CD3 treatment also displayed antileukemic activity against human CD3-positive T-ALL diagnostic cases. Mice were xenotransplanted with cells from seven distinct human T-ALL cases, five of them expressing a TCR at the cell surface, one (UPNT374) showing a heterogeneous TCR expression pattern, and the last one (UPNT525) being negative for TCR cell-surface expression. Mice were treated 24 hours later with either anti-CD3 mAb or an isotypic control antibody. For all TCR$^+$ T-ALL samples, anti-CD3 treatment showed strong antileukemic effects, as shown by delayed dissemination in blood, bone marrow, and other organs (Fig. 6A–D), an effect that translated into enhanced recipient mouse survival (Fig. 6E and Supplementary Fig. S2). In contrast, leukemic mice inoculated with TCR-negative T-ALL cells were insensitive to anti-CD3 treatment (Fig. 6B and Supplementary Fig. S2). Mice infused with UPNT374 cells only transiently responded to anti-CD3 (Fig. 6B and Supplementary Fig. S2). Interestingly, leukemic cells recovered from anti-CD3–treated

Published OnlineFirst June 28, 2016; DOI: 10.1158/2159-8290.CD-15-0675

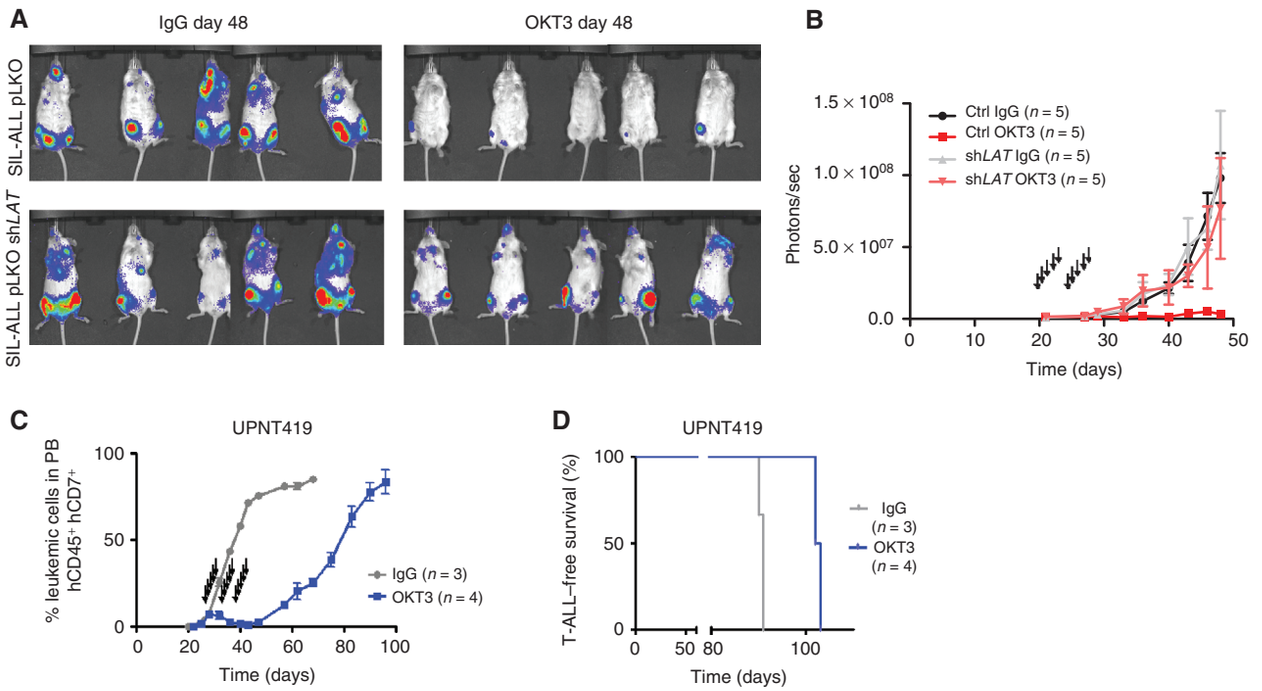

Figure 7. TCR stimulation by administration of agonistic mAb in a curative setting inhibits human T-ALL development. **A,** tumor burden in NSG mice xenotransplanted with human ALL-SIL/TCR-HY luciferase-expressing cells transduced with either the LKO control vector (top) or the LKO vector encoding *LAT* shRNA #1 (bottom). Once leukemic, mice daily received either IgG control or anti-CD3 mAb (OKT3), and bioluminescence at day 48 after xenotransplantation is shown (luminescence color scale: minimum = 8.00×10^4 to maximum = 2.00×10^6 radiance). **B,** bioluminescence quantification over time of the experiment shown in **A**. **C,** tumor burden in peripheral blood of NSG mice xenotransplanted with human T-ALL cells (UPNT419) and treated with either control IgG or OKT3 when mice were leukemic. **D,** Kaplan–Meier survival curves of NSG mice transplanted with UPNT419 analyzed in **C**.

mice showed low or absence of TCR cell-surface expression in contrast to the leukemic cells that expanded in control IgG-treated mice (Fig. 6F). This confirms the specific depletion of TCR-positive leukemic cells in response to TCR activation. We next investigated whether anti-CD3 treatment could also result in antileukemic effects in a curative setting. First, NOD/SCID/IL2Rgc$^{-/-}$ (NSG) mice were inoculated with the luciferase-expressing human ALL-SIL/TCR-HY cells and then treated with either a control or an anti-CD3 mAb when mice presented leukemia engraftment in bone marrow (day 22 after inoculation, data not shown). Comparison of the two groups by live imaging showed a specific antileukemic effect of anti-CD3 treatment (Fig. 7A, top, and 7B). To investigate whether anti-CD3 antileukemic effects were dependent upon TCR signaling, we sought to silence the expression of LAT, a critical adaptor in TCR signaling in thymocytes and mature T cells (17). shRNAs to LAT resulted in LAT expression knockdown in ALL-SIL/TCR-HY cells (Supplementary Fig. S3A) and had no effect on TCR cell-surface expression (Supplementary Fig. S3B). LAT knockdown impaired anti-CD3–induced *in vitro* apoptosis (Supplementary Fig. S3C) and antileukemic effects *in vivo* (Fig. 7A and B and Supplementary Fig. S3D and S3E). As expected, LAT expression knockdown was maintained in leukemic cells retrieved from control and anti-CD3 mAb-treated mice (Supplementary Fig. S3F). In a second experiment, mice xenotransplanted with cells from T-ALL UPNT419 were treated with the anti-CD3 or control mAb when leukemic cell burden reached 10% to 20% of bone marrow cells. Leukemia expansion was strongly delayed in anti-CD3–treated mice, in contrast to the rapid expansion of leukemic cells in control mice (Fig. 7C). Despite the reemergence of peripheral blood leukemic cells upon cessation of treatment, survival of anti-CD3–treated mice was significantly prolonged (Fig. 7D). Thus, antibody-mediated TCR engagement results in striking antileukemic effects in xenotransplanted human T-ALLs in both preventive and curative settings.

DISCUSSION

Current T-ALL therapies involve complex, often toxic chemotherapeutic regimens. Although T-ALL outcome has improved with current therapies, survival rates remain only around 50% and 70% at 5 years in adult and pediatric T-ALL, respectively (18, 19). The genetic bases of T-ALL progression and maintenance are well characterized but have not translated so far into targeted therapies (11). There is thus unmet need for new treatments to offer therapeutic options for refractory disease and to prevent relapse. We previously observed that expression of a TCR transgene in a TCR-negative T-ALL cell line can induce cell death, provided these cells are subjected to differentiation-inducing cues (20). We report here that chronic/strong TCR signaling causes massive apoptosis of primary T-ALLs that express an endogenous TCR

Published OnlineFirst June 28, 2016; DOI: 10.1158/2159-8290.CD-15-0675

and shows potent tumor-suppressive function *in vivo*. These findings call for the incorporation of TCR-directed therapies in current treatment regimens of CD3-expressing T-ALL. Muromonab-CD3 (OKT3) was approved by the FDA in 1985 for therapy of acute, glucocorticoid-resistant rejection of allogeneic renal, heart, and liver transplants (21) and was in fact the first mAb introduced in the clinic. Since then, a number of other monoclonal antibodies to CD3 were developed (22) that may prove superior to OKT3 in T-ALL treatment. Of note, encouraging response to OKT3 therapy was reported in an adult patient with an aggressive and chemotherapy-resistant T-ALL, but the basis of this response was not studied (23).

A major drawback of current chemotherapeutic regimens in T-ALL is the frequent resistance to treatment and relapse. Leukemia initiating cells (LIC) from residual disease are thought to be responsible for relapsing cases (24, 25). In addition, resistance of T-ALL to chemotherapy is in part linked to the recurrent genetic abnormalities selected during disease progression, e.g., inactivation of the *PTEN* tumor suppressor gene and the resulting activation of PI3K/AKT signaling (26, 27). Whether administration of anti-CD3 therapy during the remission phase or its association with conventional chemotherapy regimens could target LICs and/or bypass molecular mechanisms of primitive resistance represent promising directions to be explored in future prospective studies.

T cells mature in the thymus following a highly orchestrated process controlled by both cell-intrinsic (e.g., transcription factors) and cell-extrinsic (e.g., stroma-derived cytokines/chemokines) molecular cues (28, 29). Cell-surface TCRαβ expression in DP thymocytes allows recognition of specific self-MHC/peptide to transduce a positive selection signal and maturation into single-positive thymocytes. DP thymocytes not receiving this signal die through lack of stimulation, whereas those whose TCR binds too strongly to self-MHC/peptide undergo activation-induced apoptosis and negative selection (5, 30). In both situations, TCR binding to self-pMHC is the triggering event, but how TCR engagement leads to such divergent outcomes (survival and proliferation versus death) remains unclear (31). Remarkably, these two contrasting processes are driven by a TCR signaling machinery of qualitatively similar composition (30). Available evidence indicates that the difference lies in the molecular interpretation of signals of different strength, which may rely on compartmentalization of key signaling players (32), and in the induction of divergent, complex transcriptional responses (14, 33). Indeed, it has been shown that a small increase in ligand affinity for the TCR leads to a marked change in the subcellular localization (plasma membrane for negative selecting ligands vs. Golgi complex for positively selecting ones) of essential adaptors of the RAS signaling pathway. This compartmentalization induces the conversion of a small change in analogue input (affinity for ligand) into a digital output (positive vs. negative selection; refs. 32, 34). Our results show that the antileukemic activity of anti-CD3 mAb depends upon TCR signaling cues, as it was impaired upon LAT silencing in T-ALL cells. This also suggests that, in the present experimental setting, antibody dependent cell-mediated cytotoxicity (ADCC)–like responses of the host play a minor role in anti-CD3 antileukemic properties. It is likely that in patients with T-ALL eligible for anti-CD3 therapy (about half of pediatric and 30% of adult cases), ADCC-like responses will play a more important role than in immunosuppressed mice and will add therapeutic value to the intrinsic antileukemic effects of anti-CD3. In addition, in a clinical context, TCR downregulation and/or selection of a TCR-negative subclone, as observed here in a xenotransplanted T-ALL under pressure of anti-CD3 treatment, could constitute a potential escape mechanism to treatment. These findings need to be explored in clinical trials. More extensive studies on the composition and function of TCR-induced signalosomes formed in T-ALL stimulated by anti-CD3 and the identification of critical components in T-ALL of the transcriptomic signature akin to that of thymic negative selection (14, 35, 36) should provide information on the molecular pathways involved in anti-CD3–induced apoptosis in leukemic cells. These pathways could in turn constitute new pharmaceutical targets to treat T-ALL.

Although signaling from the B-cell receptor (BCR) and pre-BCR was shown to promote B-cell malignancies (37, 38), the role of TCR signaling in T-ALL has thus far remained controversial. Studies in T-ALL mouse models indicated a pro-oncogenic role for TCR signaling (39–42). However, these data were based on transgenic TCR systems, which do not reflect the expression levels and receptor diversity found among patients with T-ALL where TCR expression is heterogeneous or absent (6). Moreover, gene inactivation studies in other mouse T-cell leukemia models have shown that TCR expression is not essential for T-ALL development (43, 44). The current work demonstrates that anti-CD3–mediated activation of endogenous TCR in human T-ALL has an antileukemic function. T-ALL often arises from immature T-cell precursors before the stage of negative selection (6, 42). Consequently, contingent expression of a non–negatively selecting TCR will render T-ALL cells sensitive to TCR-activating apoptotic signals that mimic negative selection, as demonstrated here by anti-CD3 treatment *in vitro* and *in vivo*. However, during T-ALL development, it is possible that selective events enable cells to escape post-malignancy negative selection, such as loss of TCR surface expression, as found in a subset of patients with T-ALL (6) and as demonstrated here in TEL-JAK2/TCR-HY double transgenic male mice. Such leukemias could be amenable to other therapies targeting downstream TCR signaling effectors.

The dual role of developmental molecular pathways in organogenesis and tumorigenesis is increasingly recognized, the modulation of which may provide potential therapeutic opportunities (1). In line with this, experimental restoration of cell-surface expression of Igα and Igβ in Ph^+ B-ALL was also shown to result in cell death (45). In our study, we found that reactivation in TCR-positive T-ALL blasts of the lineage-specific checkpoint control normally set by TCR signaling during T-cell development displays antitumoral functions. Importantly, despite the multiple and complex oncogenic mechanisms driving T-ALL, which include antiapoptotic (46) and proproliferative (47) signaling cues, this TCR-dependent checkpoint remains switchable to induce massive tumor cell apoptosis. Thus, reactivation of similar lineage-specific developmental checkpoints in malignancies originating from other lineages and tissues could provide a novel class of therapeutic targets in cancer.

Published OnlineFirst June 28, 2016; DOI: 10.1158/2159-8290.CD-15-0675

METHODS

Mice

TEL-JAK2 mice were bred with Marilyn transgenic, RAG2-deficient or CD3ε-deficient mice (all maintained on the C57BL/6 background), as described previously (43). Swiss Nude and NSG mice were purchased from Charles River Laboratories. $IK^{L/L}$ mice, carrying two alleles of the hypomorphic IK^{L} allele (48), were a generous gift from Dr. P. Kastner (IGBMC, Strasbourg, France). Mice were maintained under specific pathogen-free conditions in the animal facilities of the Institut Curie (Orsay, France) or University of Algarve (Faro, Portugal). NSG mice were maintained under constant antibiotic treatment (Baytril 0.01% in drinking water). All experimental procedures were performed in strict accordance with the recommendations of the European Commission (Directive 2010/63/UE), French National Committee (87/848), and Portuguese authorities (Decreto-Lei n°113/2013) for the care and use of laboratory animals. Mice were euthanized when terminally ill, as evidenced by either severe dyspnea or weakness caused by leukemic dissemination in the thymus or vital organs (bone marrow, lung, and liver), respectively. For mouse leukemia transplantation assays, 0.5–2 × 10^6 leukemic cells collected from diseased female TEL-JAK2/TCR-HY, TEL-JAK2, TEL-JAK2/CD3ε$^{-/-}$, or $IK^{L/L}$ mice were intravenously injected in the tail vein of recipient 8-to-12-week-old C57BL/6 or NSG mice (for the $IK^{L/L}$ tumor) of the indicated gender and genotype and regularly monitored through peripheral blood detection of leukemic cells ($CD45.1^+CD45.2^+$TCR-Vβ6$^+$ TEL-JAK2/TCR-HY cells or $CD4^+CD8^+$ TEL-JAK2 cells). Anti-CD3ε (145-2C11) mAb or control ChromPure Syrian Hamster IgG (Jackson Immunoresearch) was diluted in sterile PBS and intravenously administered on a regimen of 20 μg/mouse/day for 5 consecutive days for the TEL-JAK2 tumors and on a regimen of 50 μg/mouse/day for 2 periods of 5 consecutive days separated by a 2-day pause for the $IK^{L/L}$ leukemia. For human leukemia xenotransplantation assays, 1 × 10^6 fresh leukemic cells obtained from primary NSG mice engrafted with patient-derived cells from T-ALL cases M106, UPNT419, UPNT420, M149, UPNT610, UPNT374, and UPNT525 were intravenously injected in 2-month-old NSG mice. These mice were injected intravenously with either anti-CD3ε OKT3 mAb (BioXCell; 40 μg/mouse/day treatment for 2 rounds of 5 consecutive days separated by a 2-day interval) or the isotype-matched (IgG2a) C1.18.4 mAb (BioXCell), both diluted in PBS. In the curative setting, mice were treated as above when leukemic cells reached 1% to 4% of blood nucleated cells. Mice were monitored weekly by flow cytometry for leukemic load (FSC^{hi}, $hCD7^+$, $hCD45^+$ cells) in peripheral blood. Statistical analyses and survival curves were calculated using Prism 5 (GraphPad). Kaplan–Meier survival curves were compared using the log-rank test. Histologic analyses were performed on paraffin-embedded sections as detailed in the Supplementary Methods.

T-ALL Patient Samples and Cell Lines

Immunophenotypic and oncogenic features of patients with T-ALL were identified as described (6, 27, 49, 50) and detailed in Supplementary Table 1. Fresh or thawed primary T-ALL samples (peripheral blood or bone marrow) obtained at diagnosis from adult and pediatric patients were used, as well as T-ALL cells xenografted in NSG mice. T-ALLs were all included within the GRAALL-2005 study, and informed consent was obtained from all patients at trial entry (trial registration ID: NCT00327678). Studies were conducted in accordance with the Declaration of Helsinki and approved by local and multicenter research ethical committees. All samples used contained ≥80% blasts. $CD4^+CD8^+$ (DP) human thymocytes were obtained and processed as described in the Supplementary Methods. The ALL-SIL cell line (DSMZ; ACC511) was grown *in vitro* and transduced as described in the Supplementary Methods. The ALL-SIL parental line and all derivatives were authenticated by short tandem repeat DNA profiling on June 10, 2016.

In Vitro TCR Stimulation by Antigen-Presenting Cells

Splenocytes were obtained from C57BL/6 female mice, subsequently irradiated (2000 rad) and preincubated with antigenic peptides at 37°C for 1 hour (peptide pulsing). Peptides used were DBY (NAGFNSNRANSSRSS), the male antigen epitope specifically recognized by Marilyn transgenic TCR-HY, at 10, 1, 0.1, 0.01, 0.001, and 0.0001 μmol/L, and OVA (ISQAVHAAHAEINEAGR), a nonspecific peptide, at 10 μmol/L. Splenocytes were then plated out in 48-well plates, without removal of peptides. ALL-SIL/TCR-HY cells were added to the coculture system at a 1:100 ratio. Control conditions were performed in parallel with non-pulsed splenocytes, DBY without splenocytes, and ALL-SIL without transgenic TCR cocultured on DBY-pulsed splenocytes. Apoptosis was analyzed by flow cytometry at day 3 of culture, as described in the Supplementary Methods.

Flow Cytometry Analysis of Leukemic Cells

Cell suspensions prepared from mouse lymphoid organs, bone marrow, or blood were stained with fluorochrome-labeled antibodies and analyzed on a FACSCalibur cytometer (BD Biosciences), as described (43). The list of antibodies used is described in the Supplementary Methods. Data were analyzed using Diva, CellQuest (BD Biosciences) and FlowJo (TreeStar) softwares.

Anti-CD3/CD28 Cell Stimulation

Short-term stimulation was performed on cells cultured in serum-free medium for at least 15 minutes at 37°C prior to stimulation. Murine anti-hCD3 mAb (OKT3, Biolegend; 20 μg/mL) was added to the cell culture on ice for 10 minutes and mAbs were then cross-linked by the addition of goat–anti-mouse antibody to a final concentration of 50 μg/mL for 15 minutes. Stimulation (0–10 minutes) was triggered by warming cells at 37°C and terminated either by cooling cells in cold PBS or fixing cells for phosphokinase array and intracellular phosphoprotein (Phosflow) assays, respectively. For prolonged stimulation, a bead-based assay was used in which cell lines were cultured in 96- or 24-well plates and exposed to 4.5-μm diameter superparamagnetic beads covalently coupled to anti-CD3 and anti-CD28 antibodies (Dynabeads Human T-Activator CD3/CD28, Invitrogen; duration of stimulation from 1 to 12 days). Prolonged stimulation of primary T-ALL cells was performed in a coculture assay with confluent OP9-DL1 in an α-MEM media supplemented with 20% FBS (Hyclone; ThermoFisherScientific), 50 μg/mL streptomycin, and 50 IU penicillin and recombinant human cytokines hFLT3L (5 ng/mL), hIL7 (2 ng/mL), and hSCF (10 ng/mL; Miltenyi). Similarly, CD3/CD28-coated beads were added to the coculture assay following the manufacturer's instructions.

Intracellular Flow Cytometry with Phosphorylation-Specific Antibodies

Stimulation of cells was terminated by fixation with prewarmed formaldehyde (Cytofix Buffer; BD Biosciences) at 37°C for 10 minutes. After cooling on ice for 1 minute, cells were pelleted at 4°C and permeabilized in 1 mL of ice-cold methanol (Perm Buffer III; BD Biosciences). After 30 minutes, cells were washed 3 times with 3 mL of PBS and resuspended in 50 μL PBS for intracellular staining with phospho-ERK1/2-Alexa647 (pT202/pY204), phospho-STAT3-Alexa488 (pY705; BD Biosciences) or phospho-AKT-Alexa647 (pS473; Cell Signaling Technology) and incubated for 20 minutes at room temperature. After washing, cells were resuspended in PBS for

Published OnlineFirst June 28, 2016; DOI: 10.1158/2159-8290.CD-15-0675

flow cytometric analysis on FACSCanto II (BD). Data were processed using Cytobank software.

Western Blot Analyses

Sample processing and analysis are described in Supplementary Methods.

Flow Cytometry Analysis of TCR Clustering

ALL-SIL/TCR-HY cells were stained with TCR Vβ6-PE mAb (BD Biosciences) for 30 minutes at 4°C and DAPI for 5 minutes at room temperature prior to stimulation and split into two samples; one sample remained unstimulated whereas the other one was stimulated by styrene beads (Polyscience) precoated with human anti-CD3ε antibody (OKT3; Biolegend) for 10 minutes at 37°C. Cells were fixed with 1% formaldehyde. Staining was analyzed using ImageStream X mkII (Amnis Merck-Millipore). Data analysis was performed using the IDEAS image analysis software (Amnis).

Phosphokinase Antibody Array Analysis and Pharmacologic Inhibition

ALL-SIL, ALL-SIL/TCR-HY cells, human DP thymocytes, and CD3-negative (UPNT525) and CD3-positive (M149) primary T-ALLs either were left unstimulated or were stimulated with CD3/CD28 mAbs for 5 minutes. Each stimulated condition was performed in replicate. Cell lysates and Proteome Profiler Human phosphokinase array (R&D Systems) were performed according to the manufacturer's protocol. Chemiluminescence was detected by ChemiDoc XRS+ (Bio-Rad). The average signal (pixel density) of duplicate spots representing each phosphorylated kinase protein was normalized with the average signal of reference positive duplicate spots of each membrane using Image Lab software (Bio-Rad). Signal ratios for selected phosphoproteins were displayed in a heat map using Treeview software. Cyclosporine A (Novartis) and PD184352 (Selleckchem) were used at 1 μmol/L. Effects were determined by analysis of apoptosis (Annexin V/PI assay) and expression of CD25 and CD69 activation markers.

Microarray Gene Expression Profiling

RNA extraction was performed for the following cells: ALL-SIL/TCRαβ-GFP cocultured on OP9-DL1 and ALL-SIL/TCRαβ-GFP without coculture. These samples were obtained as previously described (14) in duplicate, and RNA extraction was performed at an early time point before apoptosis onset (48 hours of coculture for ALL-SIL/TCRαβ-GFP). RNA hybridization was performed on Affymetrix U133 plus 2.0 microarrays. The statistical data analysis was performed with R version 2.9.0 using the "Affy" package from Bioconductor. The probe intensities were $\log_2$ transformed and normalized using Robust Multiarray Average. Identification of differentially expressed genes was performed by Significance Analysis of Microarrays, using 500 permutations and a false discovery–rate threshold of 5%. Gene Set Enrichment Analysis (GSEA) was performed using the negative selection signature described by Baldwin and colleagues (14) as gene set. GSEA was run using signal-to-noise for the ranking gene metric and 1,000 permutations. All microarray data have been submitted to the Gene Expression Omnibus database under accession number GSE65496.

Luciferase Xenograft Studies

A total of 1×10^6 control pLKO or pLKO-sh*LAT* GFP-Luciferase sorted ALL-SIL/TCR-HY cells were intravenously injected into 2-month-old NSG mice ($n = 10$). Isofluorane-anesthesized mice were intraperitoneally injected with 2.5 mg of D-luciferin (CALIPER Life Sciences) and monitored on a weekly basis to detect luciferase activity using an IVIS Spectrum (Perkin-Elmer). When leukemic cells were detected (22 days after injection), mice were treated with either OKT3 or control mAb as described above.

Disclosure of Potential Conflicts of Interest

No potential conflicts of interest were disclosed.

Authors' Contributions

Conception and design: A. Trinquand, N.R. dos Santos, C. Tran Quang, N. Ifrah, E. Macintyre, J. Ghysdael, V. Asnafi

Development of methodology: A. Trinquand, C. Tran Quang, F. Rocchetti, B. Zaniboni, F.-L. Cosset, E. Verhoeyen, F. Pflumio, N. Ifrah, D.-A. Gross, J. Ghysdael, V. Asnafi

Acquisition of data (provided animals, acquired and managed patients, provided facilities, etc.): A. Trinquand, N.R. dos Santos, C. Tran Quang, C. Da Costa de Jesus, M. Tesio, M. Dussiot, F. Pflumio, H. Dombret, J. Ghysdael, V. Asnafi

Analysis and interpretation of data (e.g., statistical analysis, biostatistics, computational analysis): A. Trinquand, N.R. dos Santos, C. Tran Quang, M. Belhocine, C. Da Costa de Jesus, L. Lhermitte, M. Dussiot, N. Ifrah, S. Spicuglia, O. Hermine, J. Ghysdael, V. Asnafi

Writing, review, and/or revision of the manuscript: A. Trinquand, N.R. dos Santos, C. Tran Quang, M. Belhocine, E. Verhoeyen, N. Ifrah, H. Dombret, L. Chatenoud, O. Hermine, E. Macintyre, J. Ghysdael, V. Asnafi

Administrative, technical, or material support (i.e., reporting or organizing data, constructing databases): A. Trinquand, E. Verhoeyen, N. Ifrah, L. Chatenoud, E. Macintyre, J. Ghysdael

Study supervision: A. Trinquand, C. Tran Quang, N. Ifrah, E. Macintyre, J. Ghysdael, V. Asnafi

Acknowledgments

We thank E. Belloir and C. Alberti for assistance with mouse husbandry, Anne Reynaud for help with blood analyses, and Charlene Lasgi from the flow-cytometry platform of the Institut Curie.

Grant Support

A. Trinquand was supported by a grant from INCa (Institut National du Cancer: "Soutien à la Recherche Translationnelle 2012"). N.R. dos Santos was supported by an FCT Investigator contract (Fundação para a Ciência e Tecnologia) and institutional support (UID/BIM/04773/2013 CBMR). This work was supported in the Necker team by grants from the Institut National du Cancer (INCa) PLBIO13-218 and PLBIO15-094, "La Ligue Contre le Cancer" and the SFCE (Société Française des Cancers de l'Enfant), la Fédération Enfants et Santé, les associations l'Etoile de Martin, Hubert Gouin "Enfance et Cancer," Les Bagouz's à Manon, Capucine, AREMIG et Thibault Briet, and la Fondation EDF; and in the Institut Curie team by funds from Institut Curie, CNRS, INSERM, INCa (PLBIO15-094), and Ligue Contre le Cancer (Comité de l'Essonne).

The costs of publication of this article were defrayed in part by the payment of page charges. This article must therefore be hereby marked *advertisement* in accordance with 18 U.S.C. Section 1734 solely to indicate this fact.

Received June 4, 2015; revised June 24, 2016; accepted June 24, 2016; published OnlineFirst June 28, 2016.

REFERENCES

1. Garraway LA, Sellers WR. Lineage dependency and lineage-survival oncogenes in human cancer. Nat Rev Cancer 2006;6:593–602.
2. Dik WA, Pike-Overzet K, Weerkamp F, de Ridder D, de Haas EF, Baert MR, et al. New insights on human T cell development by quantitative T cell receptor gene rearrangement studies and gene expression profiling. J Exp Med 2005;201:1715–23.

Published OnlineFirst June 28, 2016; DOI: 10.1158/2159-8290.CD-15-0675

3. Von Boehmer H. Deciphering thymic development. Front Immunol 2014;5:424.
4. Gascoigne NR, Palmer E. Signaling in thymic selection. Curr Opin Immunol 2011;23:207–12.
5. Klein L, Kyewski B, Allen PM, Hogquist KA. Positive and negative selection of the T cell repertoire: what thymocytes see (and don't see). Nat Rev Immunol 2014;14:377–91.
6. Asnafi V, Beldjord K, Boulanger E, Comba B, Le Tutour P, Estienne MH, et al. Analysis of TCR, pT alpha, and RAG-1 in T-acute lymphoblastic leukemias improves understanding of early human T-lymphoid lineage commitment. Blood 2003;101:2693–703.
7. Asnafi V, Beldjord K, Libura M, Villarese P, Millien C, Ballerini P, et al. Age-related phenotypic and oncogenic differences in T-cell acute lymphoblastic leukemias may reflect thymic atrophy. Blood 2004;104:4173–80.
8. Ferrando AA, Neuberg DS, Staunton J, Loh ML, Huard C, Raimondi SC, et al. Gene expression signatures define novel oncogenic pathways in T cell acute lymphoblastic leukemia. Cancer Cell 2002;1:75–87.
9. Homminga I, Pieters R, Langerak AW, de Rooi JJ, Stubbs A, Verstegen M, et al. Integrated transcript and genome analyses reveal NKX2-1 and MEF2C as potential oncogenes in T cell acute lymphoblastic leukemia. Cancer Cell 2011;19:484–97.
10. Soulier J, Clappier E, Cayuela JM, Regnault A, Garcia-Peydro M, Dombret H, et al. HOXA genes are included in genetic and biologic networks defining human acute T-cell leukemia (T-ALL). Blood 2005;106:274–86.
11. Van Vlierberghe P, Ferrando A. The molecular basis of T cell acute lymphoblastic leukemia. J Clin Invest 2012;122:3398–406.
12. Carron C, Cormier F, Janin A, Lacronique V, Giovannini M, Daniel MT, et al. TEL-JAK2 transgenic mice develop T-cell leukemia. Blood 2000;95:3891–9.
13. Lantz O, Grandjean I, Matzinger P, Di Santo JP. Gamma chain required for naive CD4+ T cell survival but not for antigen proliferation. Nat Immunol 2000;1:54–8.
14. Baldwin TA, Hogquist KA. Transcriptional analysis of clonal deletion in vivo. J Immunol 2007;179:837–44.
15. Shi YF, Bissonnette RP, Parfrey N, Szalay M, Kubo RT, Green DR. In vivo administration of monoclonal antibodies to the CD3 T cell receptor complex induces cell death (apoptosis) in immature thymocytes. J Immunol 1991;146:3340–6.
16. Witkowski MT, Cimmino L, Hu Y, Trimarchi T, Tagoh H, McKenzie MD, et al. Activated Notch counteracts Ikaros tumor suppression in mouse and human T-cell acute lymphoblastic leukemia. Leukemia 2015;29:1301–11.
17. Balagopalan L, Coussens NP, Sherman E, Samelson LE, Sommers CL. The LAT story: a tale of cooperativity, coordination, and choreography. Cold Spring Harb Perspect Biol 2010;2:a005512.
18. Huguet F, Leguay T, Raffoux E, Thomas X, Beldjord K, Delabesse E, et al. Pediatric-inspired therapy in adults with Philadelphia chromosome-negative acute lymphoblastic leukemia: the GRAALL-2003 study. J Clin Oncol 2009;27:911–8.
19. Pui CH, Evans WE. Treatment of acute lymphoblastic leukemia. N Engl J Med 2006;354:166–78.
20. Dadi S, Le Noir S, Payet-Bornet D, Lhermitte L, Zacarias-Cabeza J, Bergeron J, et al. TLX homeodomain oncogenes mediate T cell maturation arrest in T-ALL via interaction with ETS1 and suppression of TCRalpha gene expression. Cancer Cell 2012;21:563–76.
21. Smith SL. Ten years of Orthoclone OKT3 (muromonab-CD3): a review. J Transpl Coord 1996;6:109–19; quiz 20–1.
22. Martin A, Tisch RM, Getts DR. Manipulating T cell-mediated pathology: targets and functions of monoclonal antibody immunotherapy. Clin Immunol 2013;148:136–47.
23. Gramatzki M, Burger R, Strobel G, Trautmann U, Bartram CR, Helm G, et al. Therapy with OKT3 monoclonal antibody in refractory T cell acute lymphoblastic leukemia induces interleukin-2 responsiveness. Leukemia 1995;9:382–90.
24. Clappier E, Gerby B, Sigaux F, Delord M, Touzri F, Hernandez L, et al. Clonal selection in xenografted human T cell acute lymphoblastic leukemia recapitulates gain of malignancy at relapse. J Exp Med 2011;208:653–61.
25. King B, Trimarchi T, Reavie L, Xu L, Mullenders J, Ntziachristos P, et al. The ubiquitin ligase FBXW7 modulates leukemia-initiating cell activity by regulating MYC stability. Cell 2013;153:1552–66.
26. Piovan E, Yu J, Tosello V, Herranz D, Ambesi-Impiombato A, Da Silva AC, et al. Direct reversal of glucocorticoid resistance by AKT inhibition in acute lymphoblastic leukemia. Cancer Cell 2013;24:766–76.
27. Trinquand A, Tanguy-Schmidt A, Ben Abdelali R, Lambert J, Beldjord K, Lengline E, et al. Toward a NOTCH1/FBXW7/RAS/PTEN-based oncogenetic risk classification of adult T-cell acute lymphoblastic leukemia: a Group for Research in Adult Acute Lymphoblastic Leukemia study. J Clin Oncol 2013;31:4333–42.
28. Schwarz BA, Sambandam A, Maillard I, Harman BC, Love PE, Bhandoola A. Selective thymus settling regulated by cytokine and chemokine receptors. J Immunol 2007;178:2008–17.
29. Yui MA, Rothenberg EV. Developmental gene networks: a triathlon on the course to T cell identity. Nat Rev Immunol 2014;14:529–45.
30. Morris GP, Allen PM. How the TCR balances sensitivity and specificity for the recognition of self and pathogens. Nat Immunol 2012;13:121–8.
31. Hogquist KA, Jameson SC. The self-obsession of T cells: how TCR signaling thresholds affect fate 'decisions' and effector function. Nat Immunol 2014;15:815–23.
32. Daniels MA, Teixeiro E, Gill J, Hausmann B, Roubaty D, Holmberg K, et al. Thymic selection threshold defined by compartmentalization of Ras/MAPK signalling. Nature 2006;444:724–9.
33. Yachi PP, Ampudia J, Zal T, Gascoigne NR. Altered peptide ligands induce delayed CD8-T cell receptor interaction–a role for CD8 in distinguishing antigen quality. Immunity 2006;25:203–11.
34. Prasad A, Zikherman J, Das J, Roose JP, Weiss A, Chakraborty AK. Origin of the sharp boundary that discriminates positive and negative selection of thymocytes. Proc Natl Acad Sci U S A 2009;106:528–33.
35. Liston A, Hardy K, Pittelkow Y, Wilson SR, Makaroff LE, Fahrer AM, et al. Impairment of organ-specific T cell negative selection by diabetes susceptibility genes: genomic analysis by mRNA profiling. Genome Biol 2007;8:R12.
36. Schmitz I, Clayton LK, Reinherz EL. Gene expression analysis of thymocyte selection in vivo. Int Immunol 2003;15:1237–48.
37. Davis RE, Ngo VN, Lenz G, Tolar P, Young RM, Romesser PB, et al. Chronic active B-cell-receptor signalling in diffuse large B-cell lymphoma. Nature 2010;463:88–92.
38. Geng H, Hurtz C, Lenz KB, Chen Z, Baumjohann D, Thompson S, et al. Self-enforcing feedback activation between BCL6 and Pre-B cell receptor signaling defines a distinct subtype of acute lymphoblastic leukemia. Cancer Cell 2015;27:409–25.
39. Brabb T, Huseby ES, Morgan TM, Sant'Angelo DB, Kirchner J, Farr AG, et al. Thymic stromal organization is regulated by the specificity of T cell receptor/major histocompatibility complex interactions. Eur J Immunol 1997;27:136–46.
40. Cui Y, Onozawa M, Garber HR, Samsel L, Wang Z, McCoy JP, et al. Thymic expression of a T cell receptor targeting a tumor associated antigen co-expressed in the thymus induces T-ALL. Blood 2015;125:2958–67.
41. Kelly JA, Spolski R, Kovanen PE, Suzuki T, Bollenbacher J, Pise-Masison CA, et al. Stat5 synergizes with T cell receptor/antigen stimulation in the development of lymphoblastic lymphoma. J Exp Med 2003;198:79–89.
42. Strzadala L, Miazek A, Matuszyk J, Kisielow P. Role of thymic selection in the development of thymic lymphomas in TCR transgenic mice. Int Immunol 1997;9:127–38.
43. dos Santos NR, Rickman DS, de Reynies A, Cormier F, Williame M, Blanchard C, et al. Pre-TCR expression cooperates with TEL-JAK2 to transform immature thymocytes and induce T-cell leukemia. Blood 2007;109:3972–81.

Published OnlineFirst June 28, 2016; DOI: 10.1158/2159-8290.CD-15-0675

44. Klinger MB, Guilbault B, Goulding RE, Kay RJ. Deregulated expression of RasGRP1 initiates thymic lymphomagenesis independently of T-cell receptors. Oncogene 2005;24:2695–704.
45. Chen Z, Shojaee S, Buchner M, Geng H, Lee JW, Klemm L, et al. Signalling thresholds and negative B-cell selection in acute lymphoblastic leukaemia. Nature 2015;521:357–61.
46. Sanda T, Tyner JW, Gutierrez A, Ngo VN, Glover J, Chang BH, et al. TYK2-STAT1-BCL2 pathway dependence in T-cell acute lymphoblastic leukemia. Cancer Discov 2013;3:564–77.
47. Dail M, Wong J, Lawrence J, O'Connor D, Nakitandwe J, Chen SC, et al. Loss of oncogenic Notch1 with resistance to a PI3K inhibitor in T-cell leukaemia. Nature 2014;513:512–6.
48. Kirstetter P, Thomas M, Dierich A, Kastner P, Chan S. Ikaros is critical for B cell differentiation and function. Eur J Immunol 2002;32:720–30.
49. Asnafi V, Buzyn A, Le Noir S, Baleydier F, Simon A, Beldjord K, et al. NOTCH1/FBXW7 mutation identifies a large subgroup with favorable outcome in adult T-cell acute lymphoblastic leukemia (T-ALL): a Group for Research on Adult Acute Lymphoblastic Leukemia (GRAALL) study. Blood 2009;113:3918–24.
50. Bergeron J, Clappier E, Radford I, Buzyn A, Millien C, Soler G, et al. Prognostic and oncogenic relevance of TLX1/HOX11 expression level in T-ALLs. Blood 2007;110:2324–30.

Published OnlineFirst June 28, 2016; DOI: 10.1158/2159-8290.CD-15-0675

AACR American Association for Cancer Research

CANCER DISCOVERY

Triggering the TCR Developmental Checkpoint Activates a Therapeutically Targetable Tumor Suppressive Pathway in T-cell Leukemia

Amélie Trinquand, Nuno R. dos Santos, Christine Tran Quang, et al.

Cancer Discov 2016;6:972-985. Published OnlineFirst June 28, 2016.